Information Sciences 181 (2011) 450–465

Perceptually adaptive spread transform image watermarking scheme using Hadamard transform

Santi P. Maity [a,*], Malay K. Kundu [b]

[a] Dept. of Information Technology, Bengal Engineering and Science University, Shibpur, P.O. Botanic Garden, Howrah 711 103, India
[b] Machine Intelligence Unit and Center for Soft Computing, Indian Statistical Institute, 203, B. T. Road, Kolkata 700 108, India

ARTICLE INFO

Article history:
Received 18 December 2008
Received in revised form 17 September 2010
Accepted 24 September 2010

Keywords:
Hadamard transform
HVS models
Lossy compression
Negative modulation
Spread transform
Watson distance

ABSTRACT

The present paper proposes a digital image watermarking scheme using the characteristics of the human visual system (HVS), spread transform technique and statistical information measure. Spread transform (ST) scheme is implemented using the transform coefficients of both the host and the watermark signal. Watermark embedding strength is adaptively adjusted using frequency sensitivity, luminance, contrast and entropy masking of HVS model. The choice of Hadamard transform as watermark embedding domain offers several advantages, such as low loss in image information (higher image fidelity), greater reliability of watermark detection and higher data hiding capacity at high degree of compression. Performance of the proposed method is compared with a number of recently reported watermarking schemes based on spread spectrum (SS) and quantization index modulation (QIM).

1. Introduction

With the rapid development of computer and communication networks, the distribution of multimedia signals via internet in digital form become popular in recent times. This popularity is due to the open system nature of internet which incidently allows gross duplication, alteration or even stolen of data by unscrupulous intruders [10]. So the real threat of the owner of the multimedia data is how to maintain their claim of ownership, or to protect the content from an illegal manipulation. This leads to the development of techniques for authentication and protection of the data content [9].

One way to protect this ownership right, authentication and integrity verification is done by embedding additional information invisibly before the digital media is made available for the public use [2,9,10]. This embedded information is popularly known as digital watermark and it may contains information about the media, the owner, copyright or licence, etc. The data to be protected is called original or host data and the resultant data after watermarking is called watermarked data. A good watermarking algorithm must satisfy three basic properties like good degree of imperceptibility, robustness and also high data hiding capacity but without compromising for any of them [6,15,43] with others. Reversible data hiding methods are also reported in [44,7] that minimize or eliminate loss due to embedding and reconstruct host data only from stego-data. This type of data hiding finds specialized applications in law, military and medical use.

Several methods for watermarking of the multimedia signals are reported in the literature [2,5,9,29,18,23,47]. Although some recent works use non-conventional approach like properties of DNA (deoxyribonucleic acid) sequences in data hiding [41] as well as intelligent computation method like support vector machine for watermark extraction, majority of the

algorithms developed are based on two popular communication principles like spread spectrum (SS) [9,24,25,27,29] and quantization index modulation (QIM) [8,19,20]. Each one of the latter two principles not only has some relative advantages but also disadvantages too. SS watermarking is found to be efficient, robust and cryptographically secured method. But it suffers from few drawbacks like (i) poor payload capacity (due to large bandwidth requirement), (ii) residual correlation between the host and the watermark and (iii) ineffectiveness of the correlation decoder structure for incorporating the attack interference and fading operation. On the other hand, QIM watermarking does not suffer from payload and residual correlation problem and also more robust against additive noise corruption compared to SS [8]. But it also suffers from serious disadvantages like extreme sensitivity to valumetric scaling [19]and fading operation [28]. A good use of the characteristics of human visual system (HVS) in both SS [35] and QIM watermarking schemes ware implemented in [19,20] in order to achieve better imperceptibility and robustness simultaneously.

Digital image watermarking algorithms are implemented either in spatial (pixel) domain [29] or in frequency domain using different transforms such as DCT (discrete cosine transform) [2,4,9,19,42], DWT (discrete wavelet transform) and its variants [16,21,22,24,31], DFT (discrete Fourier transform) [38] and Fourier-Mellin [39], etc. Among transforms, DCT and DWT are found to be more popular for implementation of compression resilient watermarking schemes mainly due to two reasons, (i) till to date the most common image compression techniques are JPEG and JPEG 2000 which are based on DCT and DWT, respectively, (ii) also lot of results on incorporation of characteristics of HVS are already available for both these two transforms. The results influence their use in designing imperceptible data hiding schemes. It is also reported in watermarking literature [11,36,37] that most wavelet-based embedding schemes (like JPEG 2000, SPIHT, EZW, etc.) are very robust against low quality JPEG 2000 compression, but are not similarly resilient against low quality JPEG compression. Similarly, DCT based digital watermarking methods are having exactly inverse characteristics for compression operations. Ramkumar et al. [36,37] showed that discrete Hadamard transform (DHT) possesses low standard deviation for the processing noise at low quality compression. These facts may help DHT based schemes to achieve simultaneously optimum robustness against low quality compression and higher embedding capacity which show better performance compered to either DCT or wavelet based schemes. So we conjure that it may be a good attempt to use DHT and HVS characteristics for designing optimal data hiding scheme having good degree of robustness and imperceptibility. To the best of our knowledge, this integration has not yet been attempted so far.

This paper proposes a HVS based spread transform (ST) watermarking scheme using DHT. The use of DHT offers mainly twofold advantages, namely (i) binary modulation effect in data hiding that leads to better robustness against noise addition, and (ii) low visual distortion in term of Watson distance measure, when HVS characteristics with entropy masking is used. Moreover, embedding in DHT domain improves robustness against high degree (low quality) JPEG and JPEG 2000 compression with high payload capacity. In addition to that in the proposed spread transform (ST) based watermarking, the significant transform coefficients of the host image are modulated by the corresponding watermark coefficient. This data embedding approach not only improves fidelity of the watermarked image but also increases robustness comparable to SS watermarking. It is also found that proposed scheme shows improved robustness performance against fading like operations compared to many SS and QIM methods. Robustness performance of the decoded multi-valued watermark is measured using mutual information. In case of binary watermark, the measurement is done in term of bit error rate (BER). The performance of the system as envisaged by mathematical analysis is duly supported by experimental results.

The organization of the paper is as follows: Section 2 presents review of some related watermarking methods and the scope of the present work. Mathematical models and analysis are discussed in Section 3. Section 4 describes the spread transform watermarking technique. The proposed watermark embedding and decoding schemes are explained in Section 5. Sections 6 and 7 present simulation results with discussion and conclusions, respectively.

2. Review of related watermarking methods, limitations and scope of the present work

Literature on digital image watermarking is quite rich. In this section, we present a brief literature review related to recently published DCT and DWT based SS and QIM watermarking and also some HVS based image watermarking techniques. The objective of this review section is to discuss the merits and limitations of some related works and scope of the proposed work.

2.1. Review of related works

Malvar et al. [29] propose an improved version of zero-rate SS watermarking. The effect of the host signal interference is partially canceled which leads to robustness gain almost similar to that of QIM scheme against additive noise. However, performance against amplitude scaling and fading operation is not improved much.

On the other hand, Li and Cox [19] propose a perceptual model based DCT domain QIM watermarking to improve fidelity and resiliency against valumetric scaling. Suthaharan et al. [42] develop a DCT based perceptually tuned robust image watermarking scheme using HVS. Fei et al. [11] made an extensive study on the different aspects of design of SS and QIM watermarking algorithms and analyze how to achieve improved performance under lossy compression.

Lin and Lin [22] propose a wavelet-based copyright protection scheme where the secret key is generated during the embedding process using local features extracted from the perceptually prominent components of the wavelet transformed

host image. Chang et al. [7] propose a high-payload frequency-based reversible image hiding method using Haar digital wavelet (HDWT) transform followed by adaptive arithmetic coding method to encode the HDWT coefficients in a high frequency band. Paquet et al. [31] propose wavelet packet-based digital watermarking for image verification and authentication. Kumsawat et al. [16] propose an algorithm for optimization in zero-rate SS watermarking using muti-wavelet transform and genetic algorithms (GAs). The objective function of GA uses the universal quality index (UQI), which matches the HVS characteristics accurately.

On summarization of the review works, it is found that the watermarking methods reported in [19,42] offer better imperceptibility for the hidden data. However, robustness performance against low quality JPEG 2000 operation is not good enough for these methods. Similarly, the watermarking methods published in [22,16] are robust against low quality JPEG 2000 compression but could not retain good visual quality of the watermarked images. Also, they are not robust enough particularly against low quality JPEG compression. The method as proposed in [31] suffers from deficiencies like low payload capacity, computation cost increases exponentially with the increase of payload and poor robustness against low quality compression. The methods as reported in [29,11] can achieve good robustness performance on significant sacrifice of watermark payload. The reconstruction of host image in [7] from the watermarked signal transmitted through radio mobile channel at low signal-to-noise ratio is affected lot.

2.2. Scope of the work

The notable facts emerged from the above review are as follows:

(1) Dither modulation (DM) based QIM [8,19] offers greater robustness against noise addition due to binary modulation nature in data hiding. This fact is well explained in digital communication literature that binary signaling offers reliable data transmission compared to M-ary signaling [14] in noisy channel. However, QIM watermarking, in general, suffers from valumetric scaling operation.
(2) SS watermarking, although offers poor BER (bit error rate) performance against additive white Gaussian noise (AWGN) compared to QIM, but is quite robust against forced removal operations [27].
(3) HVS model based watermarking methods improve image fidelity using contrast and entropy masking [26,42].
(4) DHT may be a good candidate as working domain for embedding watermark information in order to achieve low loss in image information, good robustness against platform independent compression (JPEG or JPEG 2000) at low quality factor and with high payload capacity [36,37].

The basic objective of this work is to achieve simultaneously fairly well perceptual transparency for the hidden watermark information, high payload capacity and greater robustness against varieties of signal processing operations. These include noise addition, scaling and platform independent lossy compression at low quality factor and typical fading like operation experienced in radio mobile channel or time varying collusion attack. Selection of watermark embedding domain and modulation strategy play an important role to meet the goals. The embedding domain should possess inherent property favorable for binary data modulation. Although this two level data embedding produces low entropy value but it becomes very effective in contrast masking in HVS based model. It is also seen that two-level change produces low variance value for the watermarked region that results in reliable watermark decoding. Based on this observation, watermark embedding is done on DHT domain which has bi-level integer valued kernels. It is shown both analytically as well as by simulation experiment that DHT domain embedding offers better fidelity in term of low Watson value. Moreover, the orthogonal row-columns of DHT offer good degree of independencies among the coefficients. Watermarking on these coefficients may be looked like frequency diversity analogous to multiple independent paths in radio mobile channel and thus leads to robustness against fading operation.

3. Mathematical models and analysis

This section highlights the advantages of DHT as signal decomposition tool for watermark casting, HVS characteristics and subsequent generation of modulation functions.

3.1. DHT as signal decomposition tool for watermarking

Let us assume that watermark information is embedded separately in Hadamard coefficient and in other unitary transform, say DCT, coefficient. Let us now examine the effect of additive watermarking that changes average gray level information of the host image. We first write the expression of the host image $f(x,y)$ of size $(N \times N)$ (where $N = 2^n$) in term of Hadamard coefficients as follows [12]:

$$f(x,y) = \sum_{u=0}^{N-1}\sum_{v=0}^{N-1} H_{u,v}(-1)^{\sum_{i=0}^{n-1}[b_i(x)b_i(u)+b_i(y)b_i(v)]}. \tag{1}$$

We drop the term $1/N^2$ from Eq. (1) as it merely represents a scale factor. Accordingly, the watermarked image after data embedding by an amount Δw in $H_{j,k}$ where $j, k \neq 0$, can be written as follows:

$$f_1(x,y) = \left[H_{j,k} + \Delta w\right](-1)^{\sum_{i=0}^{n-1}[b_i(x)b_i(j)+b_i(y)b_i(k)]} + \sum_{u=0,u\neq j}^{N-1}\sum_{v=0,v\neq k}^{N-1} H_{u,v}(-1)^{\sum_{i=0}^{n-1}[b_i(x)b_i(u)+b_i(y)b_i(v)]} \tag{2}$$

where $x, y = 0, 1, 2, \ldots (N-1)$. The change in the pixel values, due to watermark embedding, can be obtained by subtracting Eq. (1) from Eq. (2) and is expressed as follows:

$$\Delta f(x,y) = \Delta w(-1)^{\sum_{i=0}^{n-1}[b_i(x)b_i(j)+b_i(y)b_i(k)]} = \pm\Delta w, \tag{3}$$

where the exponent of (-1) is **0** for half of the cases and **1** for the remaining cases, according to the property of Hadamard kernel. As a result, the pixel values are increased or decreased by Δw, respectively. The result so obtained is valid for embedding of watermark information in any coefficient with $u = l$, $v = k$ where $l, k \neq 0$.

On the other hand, if watermark information is embedded in the coefficient with $u = l$, $v = k$ where $l, k \neq 0$ for other transform, say DCT, the change in pixel values can be written similar to the Eq. (3) as follows:

$$\Delta f(x,y) = f_1(x,y) - f(x,y) = \Delta w \cos\left[\frac{(2x+1)l\pi}{2N}\right]\cos\left[\frac{(2y+1)k\pi}{2N}\right]. \tag{4}$$

Eq. (4) shows that the amount of change in the pixel values are different for different pixels. This change also depends on the selection of the particular coefficient i.e. u and v values to be used for embedding. One of the good measure to quantify the change in spatial correlation of the neighboring pixels is the average information (entropy) occurred by the change in pixel values. This average information, due to Shannon [40], is given as below

$$H = -\sum_{i=1}^{n} p_i \log p_i, \tag{5}$$

where p_i is the probability of the occurrence of the event 'i' with $0 \leqslant p_i \leqslant 1$ and $\sum_{i=1}^{i=n} p_i = 1$. Here p_i indicates the probability of the occurrence of the change in pixel values by the amount Δw_i.

The results in Eqs. (3) and (4), when put into the Eq. (5), can be summarized as follows:

Image information is changed by less amount in case of Hadamard domain embedding compared to other popular transform domain embedding as in the latter cases different pixel values of a block are changed by different amount due to the multi valued kernels.

The above mathematical analysis is well supported by the simulation results for different test images and is shown in Table 1. Furthermore, the use of Hadamard transform as signal decomposition tool offers simpler implementation (forward and inverse kernels are identical), low computation cost (as floating point multiplication and addition not required) and ease of hardware implementation (same hardware block can be used for both way implementation) [1,25]. It would not be out of point to mention here that major computation in digital signal processing (DSP) is due to multiplication operation [30] and DHT offers advantages as addition/subtraction is the key operation. The other important property is the orthogonality among the rows (and columns) of DHT. This offers good degree of independencies among the DHT coefficients. Proposed ST watermarking distribute each watermark information on those independent components and offers a form of benefit analogous to frequency diversity (multicarrier concept) used to improve receiver performance (robust watermark) in radio mobile channel.

3.2. HVS characteristics and generation of modulation functions

Any perceptual model of the human visual system (HVS) has to account a variety of perceptual phenomena, including luminance masking, frequency sensitivity and contrast masking. We further include entropy masking to obtain modified contrast masking. Hence, modulation function is developed here based on Watson visual [48] and entropy masking model [49]. Watson relates frequency sensitivity ($F_{u,v,b}$), luminance masking ($L_{u,v,b}$) and contrast masking ($C_{u,v,b}$) for each DCT coefficients according to the following relations:

Table 1
Entropy values before and after watermarking for different test images in a (8×8) blocks using DHT and DCT.

Image	Test 1		Test 2		Test 3	
	Entropy before	Entropy After DCT/DHT	Entropy before	Entropy after DCT/DHT	Entropy before	Entropy after DCT/DHT
Lena	2.96	5.26/3.70	3.62	5.78/4.23	4.96	5.90/5.10
F. boat	2.87	5.53/3.78	3.92	5.58/4.51	4.71	5.93/4.81
Bear	5.40	6.20/5.65	5.65	6.15/5.67	3.86	5.90/4.24

$$L_{u,v,b} = F_{u,v,b}\left(\frac{X_{0,0,b}}{X_{0,0}}\right)^{\alpha}, \tag{6}$$

$$C_{u,v,b} = max\left[L_{u,v,b}, |X_{u,v,b}|^{\beta_{u,v}}(L_{u,v,b})^{1-\beta_{u,v}}\right], \tag{7}$$

where $X_{0,0,b}$ is the zeroth order (DC) coefficient of the image block "b", $X_{0,0}$ is the average of all $X_{0,0,b}$'s, which corresponds to the mean luminance of the display, $X_{u,v,b}$ is the (u, v)th DCT coefficient of the block "b". The values of α and $\beta_{u,v}$ are set to 0.649 and 0.7 to control the degree of luminance sensitivity and contrast sensitivity, respectively.

We apply the same Watson model to cast (embed) watermark information in DHT as this transform also offers energy compactness like DCT. Moreover, DHT offers "sequency" effect which packs energy of the cover signal in the low and the middle frequency coefficients. The word "sequency" implies frequency interpretation equivalence and indicates the number of sign changes along each row of the Hadamard matrix. The analogy between sequency and frequency leads one to believe that most of the signal energy is packed in a particular band of sequences. This wide length of useful high magnitude middle frequency band offers better perceptual transparency and low processing noise that leads to compression resilient watermarking with high payload at low quality factor.

To include the correlation among the neighboring signal points, we represent contrast masking in term of entropy masking [49] according to the following relations:

$$V_{u,v,b} = max\left[C_{u,v,b}, |C_{u,v,b}|(E_{u,v,b})^{\gamma}\right]. \tag{8}$$

$$E_{u,v,b} = -\sum_{x\in N(X_{u,v,b})} p(x)\log p(x), \tag{9}$$

where $E_{u,v,b}$ is the entropy of $N(X_{u,v,b})$ which is set of $X_{u,v,b}$'s eight neighbors. The γ value is chosen experimentally to make $E_{u,v,b}$ value effective only when it is larger than 1.0. Since γ is associated with entropy $E_{u,v,b}$, the results of Eqs. (3) and (4) coupled with Eq. (5) when incorporated in Eqs. (8) and (9), show that $V_{u,v,b}$ values for DCT would be sometimes higher compared to DHT. We now define Watson distance in terms of the coefficients of the host and the watermarked images denoted by C_o and C_w, respectively and is given by

$$D_{wat}(c_0, c_w) = \left\{\sum_{u,v,b}\left(\frac{C_w[u,v,b] - C_o[u,v,b]}{V[u,v,b]}\right)^4\right\}^{1/4}. \tag{10}$$

As a result, it would not be surprised if DHT domain watermarking sometime offers slightly better visual quality of the watermarked images in term of low Watson distance compared to DCT, although the later transform has already proven to be efficient for source coding [48] and perceptually tuned digital watermark design [35,42]. The γ values indicate how $E_{u,v,b}$ commands over $C_{u,v,b}$ and can be adjusted to control robustness and perceptual transparency through the value of $V_{u,v,b}$. We choose γ value 0.5 after performing watermark embedding over large number of images. To develop the modulation function, we use a scaled version of the popular JPEG quantization table for frequency sensitivity. The modulation function is used for watermarking using spread-transform technique and is very briefly discussed in the next section.

4. Spread transform watermarking

Spread transform (ST) watermarking proposed by Chen and Wornell [8] is an approach to spread watermark information over many host signal elements. Instead of embedding watermark information directly into the host signal X, it is casted into the projection X^{ST} of X onto a random sequence t. The term "transform", as used by Chen and Wornell is somewhat misleading as it implies pseudo-random selection of signal component X to be watermarked [8]. On the contrary, the present method employs data embedding in projected domain. We select "τ" data elements of both the host (X) and the watermark signals and transform them by DHT to "τ" elements for each signal. The coefficients of the host and the watermark are then sorted in ascending order. This is done in order to add relatively large watermark coefficients to the corresponding significant coefficients of the host signal.

Furthermore, to maintain imperceptibility of the hidden data, suitable weighting factors are selected using HVS (perceptual model). It may be mentioned here that the integration of HVS model and spread transform in DCT domain watermarking scheme is also reported in [19,20]. This is done in order to meet fidelity as well as robustness against amplitude scaling and JPEG compression. Although, the watermarked images look good visually, but still further improvement is possible by incorporating property of entropy masking. Moreover, poor robustness performance of [19,20] against JPEG 2000 compression at low quality factor can be improved using DHT domain HVS based ST method.

The parameter "τ" may be called as *spreading factor* and the value of "τ" may be different for the host and the watermark. The term spreading factor is used here as the information embedded in x_i^{ST} will be spread over "τ" host elements by the inverse ST. The proposed ST method offers twofold spreading effect as both the host and the watermark are decomposed before embedding. The spreading effect is further improved by spatial dispersion of the message vector before projection is done. Moreover, the size of the host signals, in most cases, are larger than the auxiliary messages/watermarks and the host elements X^{ST} can be chosen with greater flexibility for data embedding. The next section describes proposed watermarking method.

5. Watermark embedding and decoding

We use in this work gray scale image as host image. The watermark signal may be a multivalued gray scale image or a binary signal. Fig. 1 shows block diagram representation of the proposed watermarking method.

5.1. Watermark embedding

Step I: Spatial dispersion of watermark image
The watermark image (W) is spatially dispersed and thus converts a gray scale or binary watermark into noise-like image. In principle, the permutation on W should cause the pixels of the watermark to be separated as far as possible. By doing so, the process helps to preserve to a certain extent the contextual information and recognize visually meaningful watermark pattern. In other words, the recovery of lost pixel values for the extracted watermark image can be made more effective.

Step II: Image transformation
The host image and the spatially dispersed watermark image are partitioned into non-overlapping blocks of size (8×8). Block based Hadamard transform is then applied over both of them. The block size is chosen as (8×8) for compatibility with JPEG compression.

Step III: Image dependent permutation
In order to increase imperceptibility of the hidden data, the transform coefficients of the host and the watermark image are sorted in ascending order so that the relatively large coefficients of the message signal/watermark will modulate the corresponding large coefficients of the host data.

Step IV: Watermarked image formation
The modulation function is formed according to the mathematical analysis as discussed in Section 3.2. Watermark information is embedded according to the following relation. If $|X_u,\ v,\ b| > V_{u,v,b}$,

$$X^m_{u,v,b} = X_{u,v,b} + sgn(X_{u,v,b}) V_{u,v,b} \frac{|Y_{u,v,b}|}{max(Y_{u,v})} \tag{11}$$

otherwise

$$X^m_{u,v,b} = X_{u,v,b},$$

where

$$sgn(X_{u,v,b}) = -1 \quad \text{if} \quad X_{u,v,b} \geqslant 0.0$$
$$= 1 \quad \text{if} \quad X_{u,v,b} < 0.0$$

The symbol $X^m_{u,v,b}$ is the data embedded (u,v)th coefficient of block "b". The symbol $X_{u,v,b}$ is the (u,v)th coefficient of the host image in block "b", $V_{u,v,b}$ is the modulation index obtained after frequency, luminance, contrast and entropy masking, $Y_{u,v,b}$ is

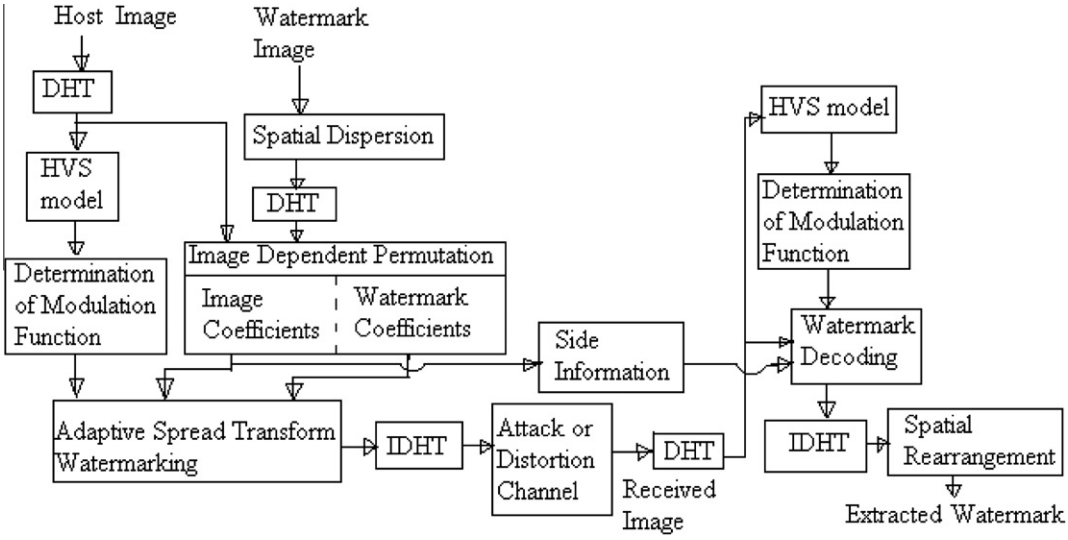

Fig. 1. Block diagram representation of the proposed watermarking scheme.

the coefficient of watermark image which is responsible to modulate $X_{u,v,b}$. The symbol $\max Y_{u,v,b}$ indicates the maximum value of the coefficients for the watermark image.

An adaptive negative modulation technique is used for data embedding [26] in order to improve robustness performance against lossy compression operation. In negative modulation, the sign of the cover image transform coefficient and the respective modulation quantity are different. On the other hand, it is called a positive modulation if the sign of the two respective coefficients are identical. Positive modulation strategy for watermark embedding preserves good visual image quality after compression operation. But at higher compression, watermark information is lost significantly. On the other hand, negative modulation strategy for watermark embedding decreases absolute values of the watermarked transformed coefficients and does not permit higher compression in order to preserve commercial value of the marked data. As a result, loss in watermark information due to quantization operation of compression is low so long watermarked image preserves its visual quality.

We define a term as **Modu** where

$$\mathbf{Modu} = sgn(X_{u,v,b})\frac{V_{u,v,b}}{maxY_{u,v,s}}. \tag{12}$$

It is observed during the experiment over large number of test images that better imperceptibility and robustness results can be achieved if we replace **Modu** by **Modu**/10, when (i) **Modu**.$|Y_{u,v,b}| > 10.0$ and **Modu** by **Modu**.3, when (ii) **Modu**.$|Y_{u,v,b}| < 3.0$.

The modification in (i) reduces the effect of visual distortion for the relatively high transform coefficients of the watermark data and the modification in (ii) improves the retrieval of the relatively smaller transform coefficients of the watermark data from the distorted watermarked image. Block based inverse Hadamard transform is then applied and the watermarked image is formed.

5.2. Watermark decoding

The decoding of watermark information is given by the following relation:

$$Y^e_{u,v,b} = X'_{u,v,b} - (X_{u,v,b}).\mathbf{Modu}, \tag{13}$$

where $X'_{u,v,b}$ values are the coefficients of the possibly distorted watermarked image, $X_{u,v,b}$ values are the coefficients of the host image and $Y^e_{u,v,b}$ are the coefficients of the extracted watermark image. It is to be mentioned here that watermark recovery process requires the host image or the side information, such as the coefficients of the host and their respective positions. Hence the proposed watermarking method is non-blind. The transform coefficients of the extracted watermark information are placed in the respective positions. Block based inverse transformation is then applied to obtain the watermark image. The extracted watermark image is then spatially rearranged following the similar operation as done in step 1 of Section 5.1.

6. Results and discussions

Performance of the proposed algorithm is presented in Section 6.1, while mathematical analysis for robustness improvement is shown in Section 6.2.

6.1. Simulation results of performance

This section describes image fidelity, robustness performance of the proposed method and comparison with other existing watermarking methods. Fig. 2 shows different watermarks with size (64×64) used to perform experiment. Fig. 2(a) is a 4 bits/pixel gray-scale image, Fig. 2(b) and (c) are 8 bits/pixel gray scale image and binary watermark, respectively. Fig. 3(a) shows test host image Lena which is a gray-scale image of size (256×256), 8 bits/pixel [51,52]. Fast Hadamard transform (FHT) based implementation requires less processing time compared to DCT and wavelet based realization. As an example, the proposed algorithm requires approximately 4.5 s using FHT, 7 s using DCT and 10.5 s using Daubechies-2 (db2) wavelet

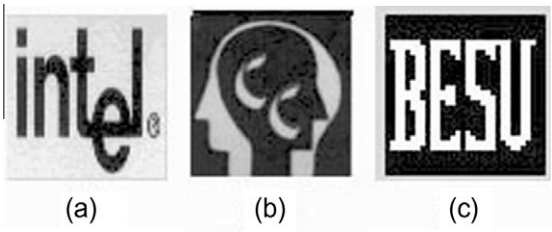

Fig. 2. (a) Watermark image of 4-bits/pixel. (b) Watermark image of 8-bits/pixel. (c) Binary watermark image.

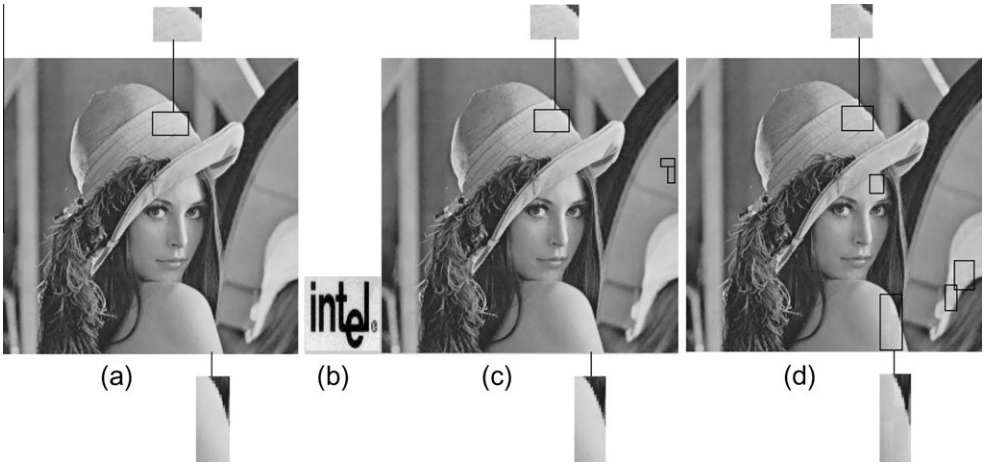

Fig. 3. (a) Host image, (b) watermark, (c) watermarked image using DHT and (d) watermarked image using DCT.

filter for watermark embedding. On the other hand, for watermark decoding, the time requirement is approximately 3 s for FHT, 4.5 s using DCT, and 6 s for wavelet (db2 wavelet basis) based methods simulated on a Pentium III 400 MHz PC system using visual C/C++.

The present study uses peak-signal-to-noise-ratio (PSNR) [12] and mean-structural-similarity index measure (MSSIM) [46] as a distortion measure for the watermarked image under inspection with respect to the original host image. Similarly, the mutual information value $I(W;W')$ and bit error rate (BER) are used as objective measure of robustness for the multilevel and binary watermark image, respectively. The symbols W and W' in $I(W;W')$ indicate random variables representing original and extracted watermark, respectively.

Fig. 3(c) and (d) show the watermarked images using DHT and DCT as signal decomposition tools, respectively. PSNR and MSSIM values between the watermarked image and the host image for DHT domain embedding are 40.02 dB and 0.9973, respectively. The respective image quality measures (PSNR and MMSIM values) for DCT domain embedding are 38.67 dB and 0.9831, respectively. The Watson distances for Fig. 3(c) and (d) are 15 and 50, respectively. The rectangular boxes shown in Fig. 3(c) and (d) indicate the areas where the visually distinguishable distortions occur. The numerical values of Watson distances are also consistent with the numerical values of other quality measures like PSNR and MSSIM.

The rectangular zoomed regions in Fig. 3(c) are quiet identical visually to the corresponding regions in Fig. 3(a). However, the regions are shown in order to highlight how the corresponding regions in Fig. 3(d) are degraded severely. On the other hand, there occurs very little distortions (almost non-noticeable) in one place on upper middle of right side broader in Fig. 3(c) which, however, is not seen in Fig. 3(d). But some visually prominent distortions are seen on few places in Fig. 3(d). The distortion occurs seemingly due to entropy masking that results from higher change in entropy in DCT domain embedding and generates relatively high Watson distance. It is to be noted here that Watson distance, unlike PSNR and MSSIM measures, is not normalized and hence how good or bad a numerical value is, also size dependent.

Table 2
Comparison of perceptual transparency for the different watermarking algorithms.

Test image	PSNR MSSIM value prop. algo	PSNR MSSIM value Suthaharan et al. [42]	PSNR MSSIM value Li and Cox [19]	PSNR MSSIM value Lin and Lin [22]	PSNR MSSIM value Kumsawat et al. [16]	PSNR MSSIM value Paquet et al. [31]
Boat	40.23 0.9981	38.34 0.9732	37.42 0.9632	36.12 0.9425	37.56 0.9521	34.56 0.9341
Bear	41.49 0.9987	39.67 0.9768	38.38 0.9534	36.24 0.9465	38.64 0.9643	35.61 0.9421
New York	39.78 0.9923	37.84 0.9645	37.64 0.9472	36.76 0.9345	37.54 0.9465	34.87 0.9402
Opera	39.56 0.9923	37.45 0.9678	37.42 0.9546	38.24 0.9621	37.68 0.9667	35.45 0.9452
Lena	40.02 0.9973	37.12 0.9621	38.38 0.9567	37.85 0.9623	38.23 0.9612	35.67 0.9524
Pill	40.12 0.9976	37.87 0.9610	38.21 0.9543	37.21 0.9436	38.23 0.9573	35.76 0.9564

We compare the visual quality of the watermarked images for the proposed algorithm with Li and Cox [19], Lin and Lin [22], Suthaharan et al. [42], Kumsawat et al. [16] and Paquet et al. [31] methods and the results are reported in Table 2. Fig. 4(a)–(e) show five other test images [51,52] used for experimentation. In all cases, payload (watermark) is of size (64×64) for comparing the perceptual transparency. In order to make compatibility in comparison, zero-rate SS watermarking scheme [16] is modified for high payload using near orthogonal binary valued pseudo noise code patterns. Results show that the proposed method always offers improved data imperceptibility compared to other watermarking methods. It is found that the proposed scheme offers best data imperceptibility compared to other perceptual methods [19,42]. One of the reasons for such outcome is due to the fact that transform coefficients of the watermark image modulate the corresponding significant transform coefficients of the host image. The DHT as signal decomposition also offers benefit of low loss in image information due to watermark embedding.

Fig. 5(a) and (c) show the watermarked images obtained after mean (PSNR value 21.41 dB) and median filtering (PSNR value 24.03 dB) operations using window sizes (11×11) and (9×9), respectively. The extracted watermark

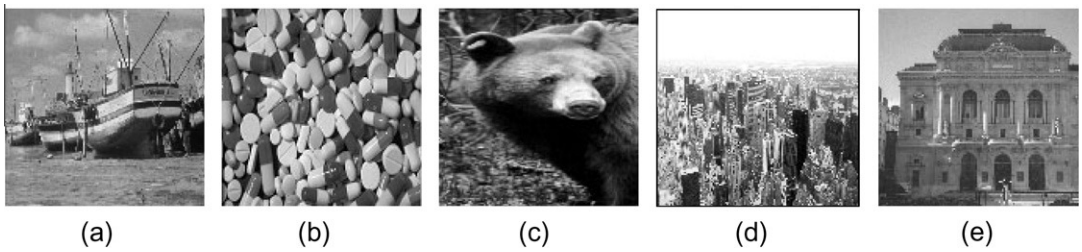

Fig. 4. Test images (a) F. boat, (b) pills, (c) bear (d) New York and (e) opera.

Fig. 5. (a) Watermarked image after mean filtering with window size (11×11), (b) extracted watermark from (a), (c) watermarked image after median filtering with window size (9×9), (d) extracted watermark from (c), (e) watermarked image after histogram equalization, (f) extracted watermark from (e).

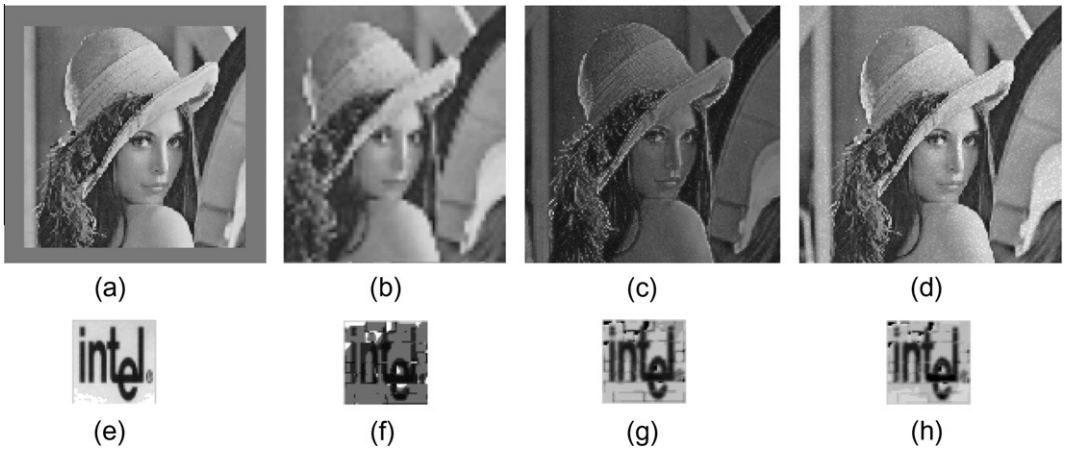

Fig. 6. (a) Watermarked image after symmetric cropping operation, (b) watermarked image after rescaling from its one-fourth size, (c) watermarked image after sharpening operation, (d) watermarked image after noise addition, (e) extracted watermark from (a), (f) extracted watermark from (b), (g) extracted watermark from (c), (h) extracted watermark from (d).

images from Fig. 5(a) and (c) are shown in Fig. 5(b)($I(W;W')$ value 0.1324) and Fig. 5(d)($I(W;W')$ value 0.1546), respectively. Fig. 5(e) shows the watermarked image (PSNR value 19.42 dB) after histogram equalization operation and the extracted watermark with $I(W;W')$ value 0.1123 is shown in Fig. 5(f). Fig. 6(a) (PSNR value 25.12 dB), (b) (PSNR value 18.34 dB), (c) (PSNR value 21.52 dB) and (d) (PSNR value 28.45 dB) show the watermarked images after symmetric cropping, rescaling, sharpening and noise addition operations, respectively. Fig. 6(e) ($I(W;W')$ value 0.1252), (f) ($I(W;W')$ value 0.0912), (g) ($I(W;W')$ value 0.0903) and (h) ($I(W;W')$ value 0.0894) show the extracted watermarks, respectively. Similarly, Fig. 7(a)–(d) show the watermarked images after wiener filtering, change in aspect ratio ($X = 1.0, Y = 1.2$), ($X = 1.2, Y = 1.0$), and rotation operations with 15^0 angle, respectively. The watermarked images have PSNR values of 22.32 dB, 27.45 dB, 27.62 dB and 22.46 dB, respectively. Fig. 7(e)–(h) show the respective extracted watermarks with their $I(W;W')$ values 0.2014, 0.1232,0.1182 and 0.1092, respectively. Fig. 8(a) (PSNR value 18.34 dB) and (c) (PSNR value 16.87 dB) show the watermarked images after JPEG and JPEG 2000 compression operations, respectively at quality factor 40. The extracted watermark images corresponding to Fig. 8(a) and (c) are shown in Fig. 8(b) ($I(W;W')$ value 0.1461) and (d) ($I(W;W')$ value 0.1256), respectively.

Robustness performance against different attacks available in StirMark 4.0 package [32–34] for the proposed as well as the other methods [16,19,22,31] are reported in Table 3. The overall performance improvement of the proposed method is due to the combined effect of spread transform and DHT. While ST scheme offers a flavor of spread spectrum, DHT offers binary modulation benefits, which is similar to dither modulation system. Moreover, DHT coefficients being relatively independent offers a form of diversity which also increases robustness. As a matter of fact, the proposed method is robust against varieties of operations.

Fig. 9(a) and (b) show graphically the robustness performance against JPEG and JPEG 2000 compression operations, respectively along with comparison with the methods in [16,19,22,42]. In all cases, we embed binary watermark of 4096 bits in (256×256) host image. Numerical results show that the methods in [19,42] offer better robustness for JPEG compared to

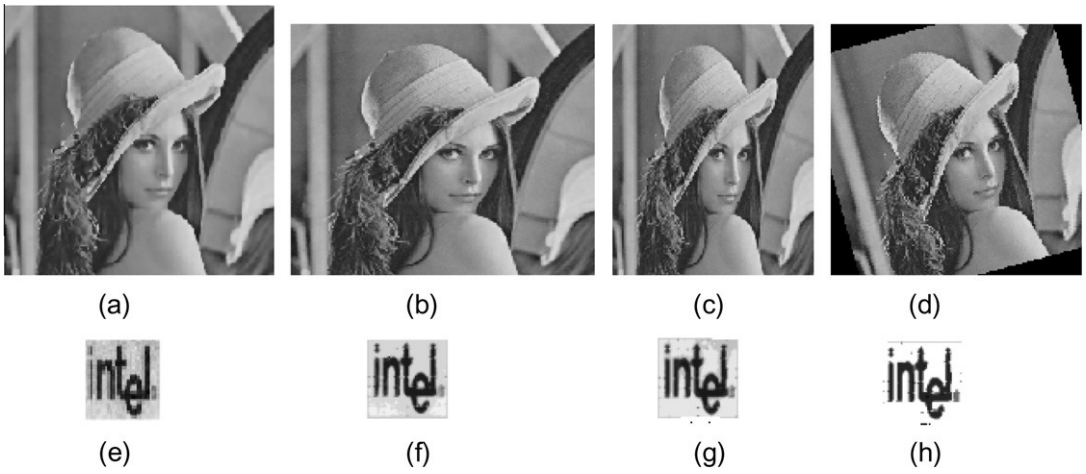

Fig. 7. (a) Watermarked image after wiener filtering with window size (5×5), (b) watermarked image after change in aspect ratio ($X = 1.0, Y = 1.2$), (c) watermarked image after change in aspect ratio ($X = 1.2, Y = 1.0$), (d) watermarked image after 15^0 rotation (e) extracted watermark from (a), (f) extracted watermark from (b), (g) extracted watermark from (c), (h) extracted watermark from (d).

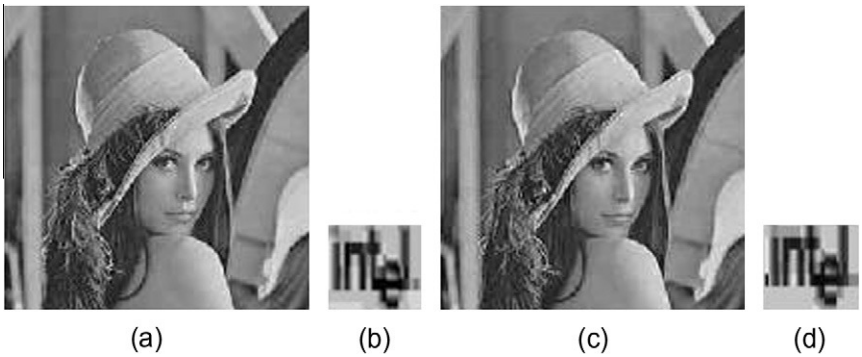

Fig. 8. (a) Watermarked image after JPEG compression at quality factor 40, (b) extracted watermark image from (a), (c) watermarked image after JPEG 2000 compression and (d) extracted watermark from (c).

[22,16] methods at low quality factor. This is quite expected as the former two are DCT based methods. It is to be noted here that the proposed method also shows comparable robustness performance similar to [19,42] methods at low quality factor. On the other hand, the methods in [22,16] offer better performance at low quality JPEG 2000 compression compared to [19,42] methods. The present method shows comparable performance similar to first two methods at low quality factor JPEG 2000. Simulation results support that the selection of Hadamard transform as signal decomposition tool shows better performance with higher payload at low quality compression compared to DCT and DWT, when both JPEG and JPEG 2000 compression operations are taken into consideration. This improved robustness performance for the proposed method is also due to negative modulation strategy used for data embedding.

We also show the sensitivity of this method to additive white Gaussian noise (AWGN) along with the methods in [16,29,19,42]. The results are shown in Fig. 10(a). As expected, the method in [16] shows the best BER performance with the increase of standard deviation of AWGN due to inherent noise immunity of QIM watermarking. On the other hand, the methods in [16,29] show relatively poor BER performance as they are developed based on SS concept and suffer from residual correlation i.e. host signal interference (HSI) problem. Among the two SS methods, algorithm [29] shows better BER performance at high standard deviation of noise, as this method removes partially HSI effect. The algorithm in [42] and the proposed method offer comparable BER performance, while the latter offers little better due to the advantage of spread transform concept. It is quite clear from the simulation results that BER performance for the proposed method against AWGN is little inferior to that of QIM method but far better than SS methods.

We also study the robustness performance of all the above watermarking methods against amplitude scaling. Watermark embedding strength for the algorithms are adjusted in such a way that PSNR values for the watermarked images are of the order of 35 dB. Once again, we find that Li and Cox [19] method offers the best BER performance against the change in scaling unlike other QIM methods that severely suffer from scaling operation. The relatively good performance of [19] method against scaling operation is due to the combination of modified Watson method, soft decoding and rational dither modulation. On the other hand [42] and the proposed one offer almost similar BER performance. At relatively high scale change, this method offers little better performance compared to [42] due to image dependent modulation for watermarking. It is interesting to note that even at scale factor 1, BER values for the extracted watermarks in [29,16] are fairly high i.e. BER performance is poor. This is due to the fact as both the algorithms were originally developed for zero-rate i.e. single bit SS watermarking and are modified here as high payload watermarking system for compatibility in performance comparison. The mutual interference among the code patterns used i.e. the cross-correlation values are highly affected due to scaling operation. This multiple bit interference effect causes inferior detection performance for both the system. Here also we see that proposed algorithm shows almost similar performance like [19] method which is resilient to scaling and offers much better BER performance compared to SS methods.

Table 3
Experimental results with StirMark 4.0 for the proposed, Kumsawat et al. [16], Li and Cox [19], Lin and Lin [22], Paquet et al. [31].

Name of attack	$I(W;W')$ value prop. algo.	$I(W;W')$ value Kumsawat et al. [16]	$(W;W')$ value Li and Cox [19]	$I(W;W')$ value Lin and Lin [22]	$I(W;W')$ value Paquet et al. [31]
Median filt. (9×9)	0.2114	0.1652	0.1758	0.1432	0.1104
Rotation-scaling 0.25	0.1244	0.0942	0.0834	0.0867	0.7562
Rotation-scaling −0.25	0.1283	0.0864	0.1143	0.0832	0.1067
Rotation-cropping 0.25	0.1537	0.1032	0.1345	0.08976	0.1134
Rotation-cropping −0.25	0.1427	0.0876	0.1956	0.1234	0.1456
Rotation (0.25)	0.1426	0.1245	0.1056	0.0789	0.1143
Rotation (5)	0.1224	0.1106	0.1056	0.0956	0.0967
Rotation (90)	0.1964	0.1256	0.1434	0.0425	0.0657
LATESTRNDDIST (1)	0.0972	0.0663	0.0578	0.0385	0.0212
LATESTRNDDIST (1.05)	0.0886	0.0131	0.0342	0.0213	0.0134
Remov-lines (10)	0.1864	0.1189	0.1056	0.0546	0.6321
Remov-lines (50)	0.1732	0.1023	0.0564	0.0234	0.0324
Remov-lines (70)	0.1715	0.1242	0.1564	0.0965	0.0732
Remov-lines (100)	0.1476	0.1127	0.1023	0.1232	0.1324
JPEG (80)	0.1657	0.1275	0.1734	0.0856	0.1423
JPEG (50)	0.1387	0.1056	0.1434	0.0345	0.0243
Cropping (50)	0.0424	0.0243	0.0123	0.0215	0.0134
Croppig (75)	0.2134	0.1689	0.0956	0.1125	0.1045
AFFINE (2)	0.1834	0.1489	0.0956	0.1145	0.1024
AFFINE (4)	0.1743	0.1345	0.1034	0.1235	0.1045
AFFINE (6)	0.1745	0.1287	0.1026	0.1015	0.1125
CONV (1)	0.1868	0.1349	0.1056	0.1023	0.1012

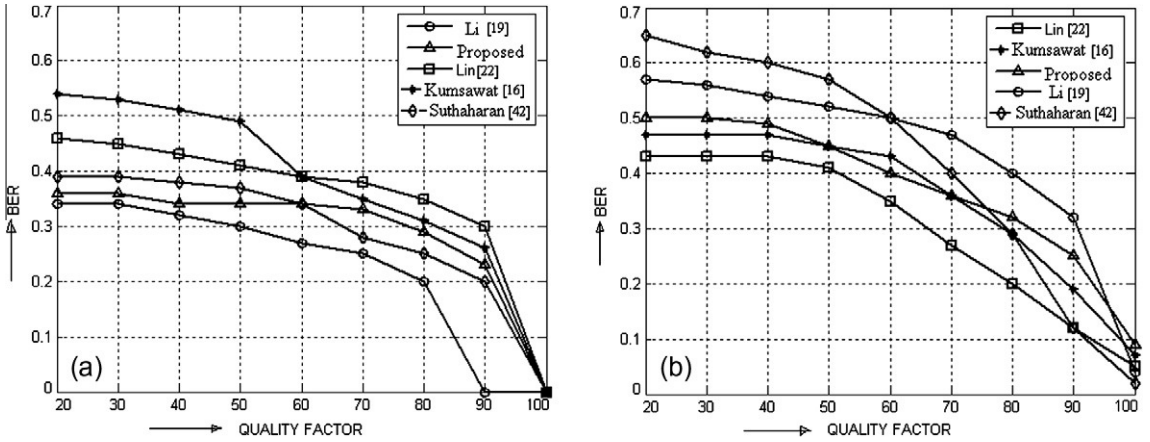

Fig. 9. BER performance against lossy (a) JPEG compression operation and (b) JPEG 2000 compression operation.

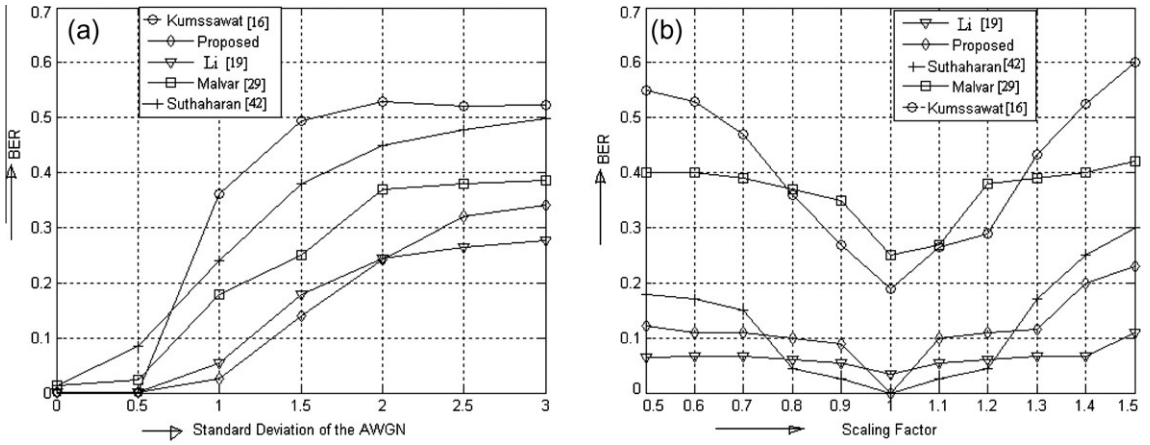

Fig. 10. BER as a function of (a) additive white Gaussian noise and (b) amplitude scaling.

Finally we study performance of this and the other methods against fading operation. The reason behind considering fading as a typical attack is due to the fact that in [17] the authors hypothesize that many common multimedia signal distortions, including cropping, filtering, and perceptual coding, are not accurately modeled as narrow band interference. They have argued that such signal modifications appear as fading like on the watermark. The widely used correlation receiver for SS watermark detection is not effective in the presence of fading like attack [17,27]. In the context of collusion attack on continuous media such as audio and video, the estimation of time varying weights become important which is analogous to different gains in fading channels. Fading in the context of wireless mobile channel means unpredictable variation in received signal strength due to vector sum of multiple copies of the same message signal received over variable path lengths [14]. During recent times, watermarking finds typical application in error concealment for image and video transmission through fading channel [28]. Transmission of watermarked data over radio mobile channel would retain watermark information provided the watermarking method is robust against fading operation.

Simulation is done here by transmitting watermarked data in Rayleigh fading channel using MC (multicarrier)-CDMA (code division multiple access) scheme [28]. Different values of signal-to-noise ratio (SNR) indicate the relative status of the wireless channel. Fig. 11(a) shows BER performance along with comparison with other methods [16,19,29,3,7]. In [3], a novel robust MC-CDMA based fingerprinting against time-varying collusion attack, which is similar to fading operation, is proposed. The algorithm uses novel communication tool sets, namely, multicarrier approach for codeword generation (Hadamard-Walsh codes are used), time varying channel response for colluder weight estimation and maximal ratio combining (MRC) detector. Graphical results shown in Fig. 11(a) reveal the fact that proposed watermarking scheme offers improved BER performance compared to all other methods except [3]. The slightly better performance of [3] is due to parallel interference cancelation for the embedded messages and this performance improvement is achieved at the cost of much increased computation cost for decoding $\sim O(n^2)$ (where 'n' is the number of embedded watermark bits). Proposed algorithm offers almost similar BER performance but at much lower computation cost due to MC-spread spectrum flavor which is the

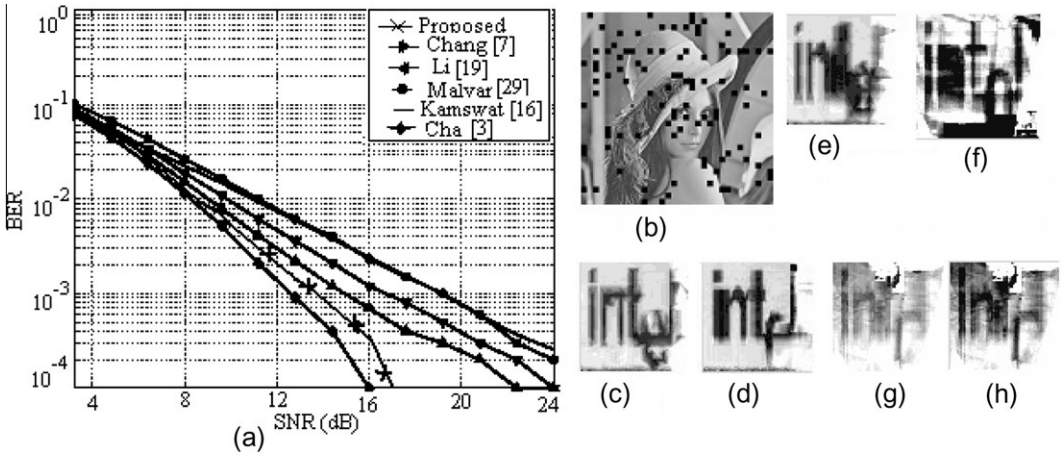

Fig. 11. (a) BER performance comparison as variation with SNR values, (b) representative watermarked image received through fading channel at SNR = 6 dB, (c)–(h) extracted watermarks for [3], proposed, [19,7,29,16].

result of combination of spread transform technique and independencies among Hadamard coefficients. The relative poor performance of other methods is due to the absence of diversity concept which in one form or other is a potential tool of improved detection performance against fading channel (operation). Relative performance shown in Fig. 11(a) is also reflected by the visual quality of the extracted watermarks shown in Fig. 11(c)–(h). Fig. 11(b) shows one representative form of the received watermarked image (using proposed watermarking scheme) transmitted through Rayleigh fading channel at SNR 6 dB. It is expected that similar degraded watermarked images (using other watermarking methods) would be received under the same channel state condition. The watermark images are extracted from the corresponding degraded watermarked images and they are shown in Fig. 11(c)–(h), respectively. It is seen that although Cha and Jay Kuo [3] method offers relatively better performance compared to proposed method against fading operation but the former shows worse performance against valumetric scaling, additive noise, low quality lossy JPEG and JPEG 2000 compression operations compared to the former.

6.2. Mathematical analysis for robustness improvement

The following two subsections show mathematically how DHT improves robustness compared to DCT or other multi-valued kernels.

6.2.1. Robustness analysis for multivalued watermark

We will now show that $I(W;W')$ values for the extracted watermarks with respect to the original one are always high in case of DHT domain implementation compared to DCT domain, after some signal processing operations (attacks) applied on the watermarked signal. The mathematical form of $I(W;W')$ [10] can be written as

$$I(W;W') = H(W) - H(W/W'), \tag{14}$$

where $H(W)$ and $H(W/W')$ indicate entropy and conditional entropy, respectively. Let us assume that jth pixel value of the decoded and the embedded watermarks are related as $w'_j = w_j + \Delta w_j$, where Δw_j is the amount of change in jth pixel values. We denote here $w_j(u)$ as jth transform coefficient of watermark, while $w_j(x)$ or simply w_j represents jth pixel value of the watermark image. We write entropy $H(W/W')$ in terms of conditional probabilities and joint probabilities [13,40] as follows:

$$H(W/W') = \sum_i \sum_j p\left(w_i, w'_j\right) \log \frac{1}{p\left(w_i/w'_j\right)} \text{(in absence of attack)}, \tag{15}$$

$$= \sum_i \sum_j p(w_i, \Delta w'_j) \log \frac{1}{p(w_i/\Delta w'_j)} \text{(in presence of attack)}. \tag{16}$$

The conditional probabilities $p(w_i/w'_j)$ or $p(w_i/\Delta w'_j)$ can be obtained from the channel matrices as shown below:

$$\begin{pmatrix} p(w'_0/w_0) & p(w'_1/w_0) \dots p(w'_{M-1}/w_0) \\ p(w'_0/w_1) & p(w'_1/w_1) \dots p(w'_{M-1}/w_1) \\ \vdots & \vdots \\ p(w'_0/w_{M-1}) & p(w'_1/w_{M-1}) \dots p(w'_{M-1}/w_{M-1}) \end{pmatrix} \text{(in absence of attack)}$$

and

$$\begin{pmatrix} p(\Delta w'_0/w_0) & p(\Delta w'_1/w_0)\ldots p(\Delta w'_{M-1}/w_0) \\ p(\Delta w'_0/w_1) & p(\Delta w'_1/w_1)\ldots p(\Delta w'_{M-1}/w_1) \\ \vdots & \vdots \\ p(\Delta w'_0/w_{M-1}) & p(\Delta w'_1/w_{M-1})\ldots p(\Delta w'_{M-1}/w_{M-1}) \end{pmatrix} (\text{in presence of attack}).$$

If there is no attack distortion i.e. no loss in watermark transform coefficient $w(u)$, we can write for the watermark pixel values as $w'_j = w_j$ irrespective of the choice of transform for decomposition of watermark signal. Thus all the elements of the upper channel matrix will have either of the two values; $p(w'_j/w_i) = p(w_j/w_i) = 0$ when $j \neq i$, otherwise '1'. The value of $H(W/W')$ is '0' (zero) and the value of $I(W;W')$ is equal to $H(w)$ according to Eq. (14).

Let us assume that jth transform coefficient of watermark signal $w_j(u)$ is changed by $\Delta w_j(u)$ due to some signal processing operation. Under such situation, it is more appropriate to calculate the value of $H(W/w')$ using Eq. (16) and the conditional probabilities from the last channel matrix (in presence of attack). According to Eq. (3), as the watermark pixel values are changed by Δw_j for all "i", $p(\Delta w'/w_i)$ values of channel matrix are finite and non-zero for all "i" i.e. only a particular column corresponding to $\Delta w'_j$ of lower channel matrix will have finite and non-zero values. On the other hand, for similar situation and in case of DCT (according to Eq. (4)), it is expected that most of the elements, if not all, of the channel matrix i.e. the conditional probabilities $p(\Delta w_j/w_i)$ for the lower channel matrix would be non-zero and finite for all combination of "i" and "j". So the value of $H(W/W')$ will be larger in case of DCT or other multivalued kernels compared to DHT. This in turn shows, according to Eq. (14), that $I(W;W')$ value is higher for DHT domain embedding compared to DCT or any multivalued kernel based embedding method.

6.2.2. Robustness analysis for binary watermark

The results of Eqs. (3) and (4) show that the effect of embedding process may be thought as analogous to M-ary pulse amplitude modulation (PAM), where DHT domain embedding indicates $M = 2$ value and higher values of M indicate the same operation for DCT or other multi-valued kernel based method.

The probability of error P_e, for more general case of M-PAM signaling [45], is expressed as:

$$P_e = \frac{2(M-1)}{M} Q\left(\sqrt{Nd_0^2/4\sigma_x^2}\right), \tag{17}$$

where 'N' indicates repetition of watermark (spreading factor τ), σ_x^2 is the variance for the change in pixel values of the host image due to watermark embedding, 'M' is the number of levels in which the transform coefficients change due to embedding. This mathematical expression shows that DHT domain embedding offers twofold benefits for detection improvement compared to DCT. The first benefit is achieved due to "M" value, which is 2 for DHT and higher for DCT or multi-valued kernel and leads to lower p_e value for the former compared to later. The second benefit is achieved from the lower variance (σ_x^2) of DHT coefficients compared to DCT coefficients. This in turn shows that argument of 'Q'-function in Eq. (17) is higher in case of DHT domain embedding compared to DCT domain embedding and leads to lower p_e value for the former compared to latter. This improvement in BER performance can also be shown in other way. The watermarking process can be analysed as communication channel, where the watermark is the signal and the host image is the noise. The simplest communication model is the additive white Gaussian noise (AWGN) channel that has the capacity C [10,50] defined by

$$C = \frac{1}{2} log_2(1 + S/N) = \frac{1}{2} log_2\left(1 + \frac{\sigma_w^2}{\sigma_X^2}\right), \tag{18}$$

where S and N are the signal (watermark) and noise (host) variances i.e. σ_w^2 (watermark power) and σ_X^2 (host signal power), respectively. Since variance of DHT coefficients is lower compared to DCT coefficients, for the same data hiding capacity, watermark power for DHT can be made much higher compared to watermark power in case of DCT. This higher watermark power helps to achieve greater robustness for DHT domain embedding compared to DCT.

7. Conclusions

The paper describes a perceptually adaptive and robust watermarking in digital images. The use of HVS characteristics and spread transform approach improves resiliency against various unintentional as well as deliberate attacks. The algorithm shows superiority in terms of robustness similar to SS watermarking scheme and data imperceptibility like perceptual based approaches. The use of fast Hadamard transformation not only reduces the computation cost due to its simplicity of kernel but also improves robustness against platform independent lossy compression which is further improved by attack adaptive negative modulation scheme. It is also shown that for a given embedding strength i.e. watermark power, Hadamard domain embedding causes smaller change in image information that results low Watson distance and better robustness compared to DCT and wavelet domain embedding. All these facts are duly verified by the standard bench marking software accepted internationally.

References

[1] A. Amira, S. Chandrasekaran, Power modeling and efficient FPGA implementation of FHT for signal processing, IEEE Transaction on Very Large Scale Integration (VLSI) Systems 15 (2007) 86–295.
[2] P. Campisi, M. Carli, G. Giunta, T. Neri, Blind quality assessment for multimedia communications using tracing watermarking, IEEE Transaction on Signal Processing 51 (2003) 996–1002.
[3] B.-Ho. Cha, C.-C. Jay Kuo, Robust MC-CDMA-based fingerprinting against time-varying collusion attacks, IEEE Transactions on Information Forensics and Security 4 (3) (2009) 302–317.
[4] C.-C. Chang, C.-C. Lin, C.-S. Tseng, W.-L. Tai, Reversible hiding in DCT-based compressed images, Information Sciences 177 (2007) 2768–2786.
[5] C.-C. Chang, W.-C. Wu, Y.-H. Chen, Joint coding and embedding techniques for multimedia images, Information Sciences 178 (2008) 543–3556.
[6] C.C. Chang, P.Y. Lin, J.S. Yeh, Preserving robustness and removability for digital watermarks using subsampling and difference correlation, Information Sciences 179 (13) (2009) 2283–2293.
[7] C.C. Chang, P.Y. Pai, C.M. Yeh, Y.K. Chan, A high payload frequency-based reversible image hiding method, Information Sciences 180 (2010) 2286–2298.
[8] B. Chen, G.W. Wornell, Quantization index modulation: a class of provably good methods for digital watermarking and information embedding, IEEE Transaction on Information Theory 47 (2001) 1423–1443.
[9] I.J. Cox, J. Kilian, T. Leighton, T. Shamoon, Secure spread spectrum watermarking for multimedia, IEEE Transaction on Image Processing 6 (1997) 1673–1687.
[10] J. Eggers, B. Girod, Informed Watermarking, Kluwer Academic Publishers, Boston, 2002.
[11] C. Fei, D. Kundur, R.H. Kwong, Analysis and design of watermarking algorithms for improved resistance to compression, IEEE Transaction on Image Processing 13 (2004) 126–154.
[12] R.C. Gonzalez, R.E. Woods, Digital Image Processing, Addison-Wesley, New York, 1992.
[13] R.H. Hamming, Coding and Information Theory, Prentice-Hall, Inc., Englewood Cliffs, New Jersey, 1980.
[14] S. Haykin, Communication Systems, fourth ed., John Wiley & Sons, Singapore, 2001.
[15] C.H. Huang, J.L. Wu, Fidelity-guaranteed robustness enhancement of blind detection watermarking schemes, Information Sciences 179 (6) (2009) 91–808.
[16] P. Kumsawat, K. Attakitmongcol, A. Srikaew, A new approach for optimization in image watermarking by using genetic algorithms, IEEE Transaction on Signal Processing 53 (2005) 4707–4719.
[17] D. Kundur, D. Hatzinakos, Diversity and attacks characterization for improved robust watermarking, IEEE Transactions on Signal Processing 29 (2001) 23832396.
[18] Y. Lee, H. Kim, Y. Park, A new data hiding scheme for binary image authentication with small image distortion, Information Sciences 179 (2009) 3866–3884.
[19] Q. Li, I.J. Cox, Using perceptual models to improve fidelity and provides resistance to valumetric scaling for quantization index modulation watermarking, IEEE Transaction on Information Forensics and Security 2 (2007) 127–139.
[20] Q. Li, I.J. Cox, Improved spread transform dither modulation using a perceptual model: robustness to amplitude scaling and JPEG compression, in: Proceedings of IEEE International Conference on Acoustics, Speech and Signal Processing (ICASSP), 2007.
[21] L. Li, X. Yuan, Z. Lu, J.S. Pan, Rotation invariant watermark embedding based on scale-adaptive characteristic region, Information Sciences 180 (2010) 2875–2888.
[22] T.C. Lin, C.M. Lin, Wavelet-based copyright-protection scheme for digital images based on local features, Information Sciences 179 (2009) 3349–3358.
[23] C.C. Lin, S.C. Chen, N.L. Hsuech, Adaptive embedding technique for VQ-compressed images, Information Sciences 179 (1–2) (2009) 40–149.
[24] S.P. Maity, M.K. Kundu, T.S. Das, Robust SS watermarking with improved capacity, Pattern Recognition Letters (Advances in Visual Information Processing) 28 (2007) 350–356.
[25] S.P. Maity, M.K. Kundu, S. Maity, Dual purpose FWT domain spread spectrum image watermarking in real-time (Special issues: circuits and systems for realtime security and copyright protection of multimedia), Comput. Electr. Eng. 35 (2009) 415–433.
[26] S.P. Maity, M.K. Kundu, An image watermarking scheme using HVS characteristics and spread transform, Proceedings of 17th International Conference of Pattern Recognition (ICPR), vol. 4, IEEE CS Press, Cambridge, UK, 2004, pp. 869–872.
[27] S.P. Maity, S. Maity, Multistage spread spectrum watermark detection technique using fuzzy logic, IEEE Signal Processing Letters 16 (2009) 45–248.
[28] S.P. Maity, S. Maity, J. Sil, Multicarrier spread spectrum watermarking for secure error concealment in fading channel, Special issue of Springer Telecommun. J., in press, doi:10.1007/s11235-010-9369-0.
[29] H.S. Malvar, D.A.F. Florencio, Improved spread spectrum watermarking: a new modulation technique for robust watermarking, IEEE Transactions on Signal Processing 51 (2003) 898–905.
[30] S.K. Mitra, Digital Signal Processing – A Computer-based Approach, Tata Mcgraw Hill, New Delhi, India, 2001.
[31] A.H. Paquet, R.K. Ward, I. Pitas, Wavelet packet-based digital watermarking for image verification and authentication, Signal Processing 83 (2003) 2117–2132.
[32] F.A.P. Petitcolas, Watermarking schemes evaluation, IEEE Transaction on Signal Processing 17 (2000) 58–64.
[33] F.A.P. Petitcolas, R.J. Anderson, M.G. Kuhn, Attacks on copyright marking systems, in: Proceedings of Second International Workshop on Information Hiding, Lecture Notes in Computer Science, vol. 1525, 1998, pp. 219–239.
[34] <http://www.petitcolas.net/fabien/watermarking/stirmark/>.
[35] C.I. Podilchuk, W. Zeng, Image adaptive watermarking using visual models, IEEE Journal on Selected Areas in Communication 16 (1998) 525–539.
[36] M. Ramkumar, A.N. Akansu, Capacity estimates for data hiding in compressed images, IEEE Transaction on Image Processing 10 (2001) 1252–1263.
[37] M. Ramkumar, A.N. Akansu, A. Atlanta, On the choice of transforms for data hiding in compressed video, IEEE ICASSP 6 (1999) 3049–3052.
[38] J.O. Ruanaidh, T. Pun, Rotation, scale and translation invariant digital image watermarking, in: Proceedings of the ICIP 1, Atlanta, GA, 1997, pp. 536–539.
[39] J.O. Ruanaidh, T. Pun, Rotation, scale and translation invariant spread spectrum digital image watermarking, Signal Processing 66 (1998) 303–317.
[40] C.E. Shannon, A mathematical theory of communication, Bell System Technical Journal 27 (1948) 379–423.
[41] H.J. Shiu, K.L. Ng, J.F. Fang, R.C.T. Lee, C.H. Huang, Data hiding methods based upon DNA sequences, Information Sciences 180 (2010) 2196–2208.
[42] S. Suthaharan, S.W. Kim, H.K. Lee, S. Sathananthan, Perceptually tuned robust watermarking scheme for digital images, Pattern Recognition Letters 21 (2000) 45–149.
[43] H. Tsai, D. Sun, Color image watermark extraction based on support vector machines, Information Sciences 177 (2007) 550–569.
[44] H.W. Tseng, C.P. Hseieh, Prediction based reversible data hiding, Information Sciences 179 (2009) 2460–2469.
[45] S. Voloshynovskiy, T. Pun, Capacity-security analysis of data hiding technologies, in: Proceedings of the IEEE International Conference On Multimedia and Expo ICME2002, Lausanne, Switzerland, August 26–29, 2002.
[46] Z. Wang, A.C. Bovik, H.R. Sheikh, E.P. Simoncelli, Image quality assessment: from error measurement to structural similarity, IEEE Transaction on Image Processing 13 (2004) 1–14.
[47] F.-H. Wang, K.K. Yen, L.C. Jain, J.-S. Pan, Multiuser-based shadow watermark extraction system, Information Sciences 177 (2007) 2522–2532.
[48] A.B. Watson, DCT quantization matrices visually optimized for individual images, in: Proceedings of the SPIE Conference on Human Vision, Visual Processing, and Digital Display IV, vol. 1913, 1993, pp. 202–216.

[49] A.B. Watson, R. Borthwick, M. Taylor, Image quality and entropy masking, in: Proceedings of the SPIE Conference on Human Vision, Visual Proc. and Digital Display VI, 1997.
[50] F. Zhang, Z. Pan, K. Cao, F. Zheng, F. Wu, The upper and lower bounds of the information-hiding capacity of digital images, Information Sciences 178 (2008) 2950–2959.
[51] <http://www.cl.cam.ac.uk/fapp2/watermarking>.
[52] <http://sipi.use.edu/services/database/Database/html>.